A PETROPHYSICAL AND SHALLOW GEOPHYSICAL STUDY TO DETERMINE PATHWAYS OF GAS MIGRATION WITHIN AND ABOVE AN UNDERGROUND GAS STORAGE FIELD IN NORTH-CENTRAL ILLINOIS

LAUREN I. HUNT

57 Pages

July 2004

A seismic survey, borehole data, and well log data were used to determine the properties of the formations within and above the reservoir and delineate possible gas migration pathways.

APPROVED:

Date	Eric W. Peterson, Chair
Date	David Malone
Date	Robert S. Nelson

A PETROPHYSICAL AND SHALLOW GEOPHYSICAL STUDY TO DETERMINE PATHWAYS OF GAS MIGRATION WITHIN AND ABOVE AN UNDERGROUND GAS STORAGE FIELD IN NORTH-CENTRAL ILLINOIS

LAUREN I. HUNT

57 Pages August 2005

The purpose of this study is to delineate the probable pathways of gas migration within and above a gas storage reservoir in North-Central Illinois. Mud logs and recorded formation tops were used to determine formation properties. A seismic survey with both P-wave and SH-wave and well log analysis including density porosity and gamma ray logs were utilized to define the gas migration pathways. The SH-wave seismic survey area included all of the surficial area utilized in the injection and withdrawal of the gas, the gathering system and areas to both the east and west. The P-wave seismic survey covered some of the same areas as the SH-wave, but not all. Gamma ray logs from numerous wells within the gas storage field including both production and observation wells were analyzed to determine the volume of shale (Vsh) within each of the formations and units within the reservoir. Three newly installed and logged wells provided the density porosity curves needed to analyze each formation

within and above the reservoir. Finally, due to the age of the gathering system and the results from all of the above, it was found that the gas could be migrating to the surface or surficial bedrock by way of faults and fractures or mechanical problems within the wells themselves.

APPROVED:

Date	Eric W. Peterson, Chair
Date	David Malone
Date	Robert S. Nelson

A PETROPHYSICAL AND SHALLOW GEOPHYSICAL STUDY TO DETERMINE PATHWAYS OF GAS MIGRATION WITHIN AND ABOVE AN UNDERGROUND GAS STORAGE FIELD IN NORTH-CENTRAL ILLINOIS

Lauren I. Hunt

A Thesis submitted in Partial
Fulfillment of the Requirements
for the Degree of

MASTER OF SCIENCE

Department of Geography-Geology

ILLINOIS STATE UNIVERSITY

ACKNOWLEDGEMENTS

The writer wishes to thank many people for their contributions of time, assistance, money, and data acquisition and processing. First of all, I would like to thank my thesis advisors, Eric Peterson, Robert Nelson and David Malone. I would also like to thank Nicor personnel, Kevin Schofield, Joe Deters, Steve Botten, Art Sanders, Sharon Ashenbrenner, Andrew Hammerschmidt, Mike Fugate, Dean Whilhelm, and all of the other people that were helpful during this whole process. Many others in industry also contributed advice in engineering, data processing, and computer navigation. They were Andre Pugin, Illinois State Geological Survey, Hannes Leetaru, Illinois State Geological Survey, Ted Kronas, Peoples Energy, Ken Moss, Baker Atlas, Dave Jacobson, Baker Atlas, and Mike Everts, Landmark. I would also like to thank my seismic data acquisition crew from Illinois State University, Tim Walls, John McEvoy, Julia Ferguson, Evan Bowen, Dean Frohling, Chris Ball, and Josh White. Also, from Illinois State University Bill Shields helped with computer troubleshooting.

L. I. H.

CONTENTS

TABLES

FIGURES

CHAPTER I

INTRODUCTION AND HYPOTHESIS

Introduction

Natural gas (methane) is used for many purposes including residential, commercial, industrial, vehicle fuel, electric power, and lease and plant fuel at the gas storage field itself. Since the 1915, natural gas has been stored in geologic formations in order to meet the needs of homes and businesses during the winter months. Even though natural gas is used all year around, the majority of consumption occurs during the winter. Originally stored in tanks, large balloons within steel structures, natural gas stored below the surface is safer and more economical. Natural gas is stored in three different types of underground sites, salt caverns, aquifers, and depleted oil and gas reservoirs (Figure 1). There have been attempts to utilize abandoned mines and hard rock caverns, but both are still in the testing stages. Underground gas storage is common all over the United States, but is more popular in the Midwest and the Northeast (Figure 2) (EIA, 2004). In north-central Illinois aquifers are the facility of choice because there is a lack of salt caverns and depleted oil and gas reservoirs (Figure 2). The total capacity of gas storage fields within the United States has risen over the last 20 years from 4,898,000 million cubic feet (Mcf) in 1973 to 8,216,397 Mcf in 2004 (EIA, 2005).

Nicor, Inc., formerly Northern Illinois Gas Company, is the premiere natural gas provider for the northeast portion of Illinois. Nicor has seven underground natural gas storage fields, one of which is in north-central Illinois near LaSalle, Illinois. In north-

central Illinois, natural gas is stored within the Cambrian Eau Claire Formation and Mt. Simon Sandstone. The storage facility is intended to hold at least 35 billion cubic feet (bcf) of natural gas and as much as 78 bcf. The pressures in the reservoir range from 375 to 750 bottom hole pressure pounds per square inch absolute (bhpsia) annually. Pressures within any underground gas storage facility where gas is stored in an aquifer are determined by the aquifer before injection. Prior to emplacement, the pressure in the aquifer was 610 bhpsia (Deters, et al., 2003).

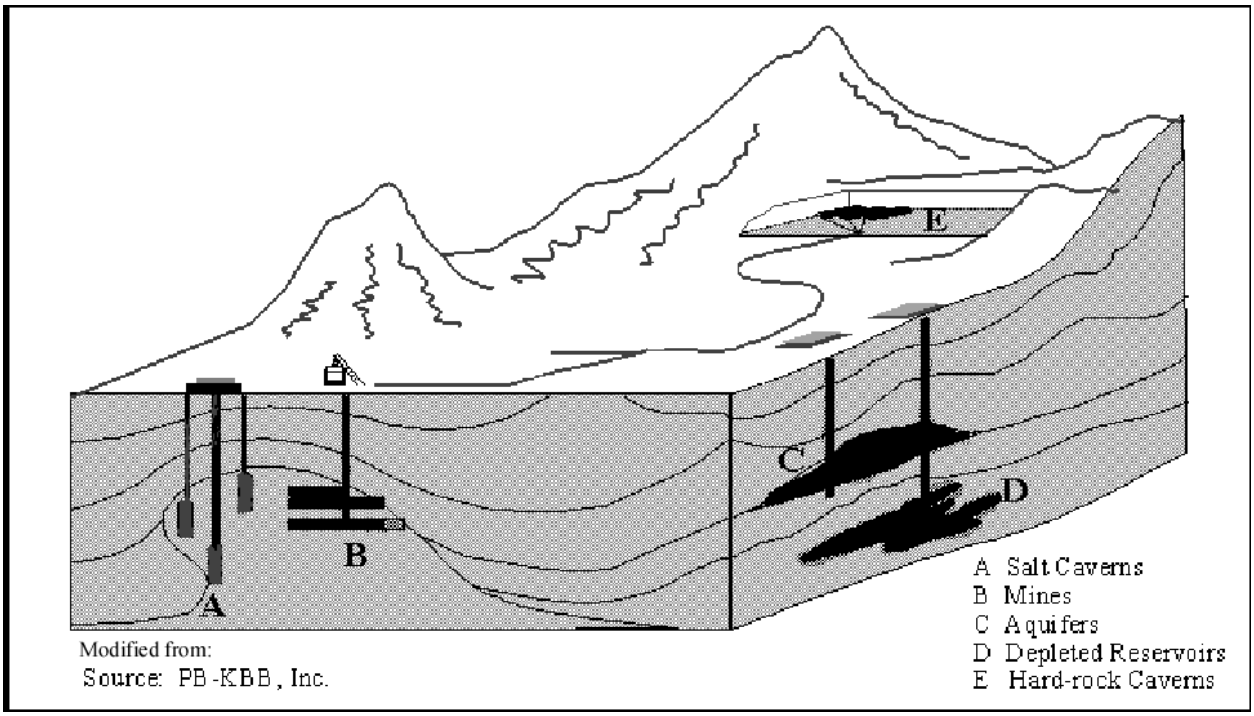

Figure 1: Types of Underground Natural Gas Storage Facilities

The process of storing natural gas is complex. The gas is brought in by pipeline and injected into the aquifer through injection/withdrawal wells. Injection at Troy Grove usually runs from May to late October. Withdrawal begins when demand exceeds

pipeline capacity. The reservoir and flow pressure are monitored on a daily basis. This information allows the reservoir engineer determine if flow rates and pressures are where they should be for that time of year. Also, the data ensures the safety of those working and living in the area. For instance, the reservoir needs to be at a certain pressure and inventory each week and month during injection to reach maximum capacity by the winter. However, exceedingly high pressures could indicate problems within the reservoir or gathering system (Deters et al., 2003).

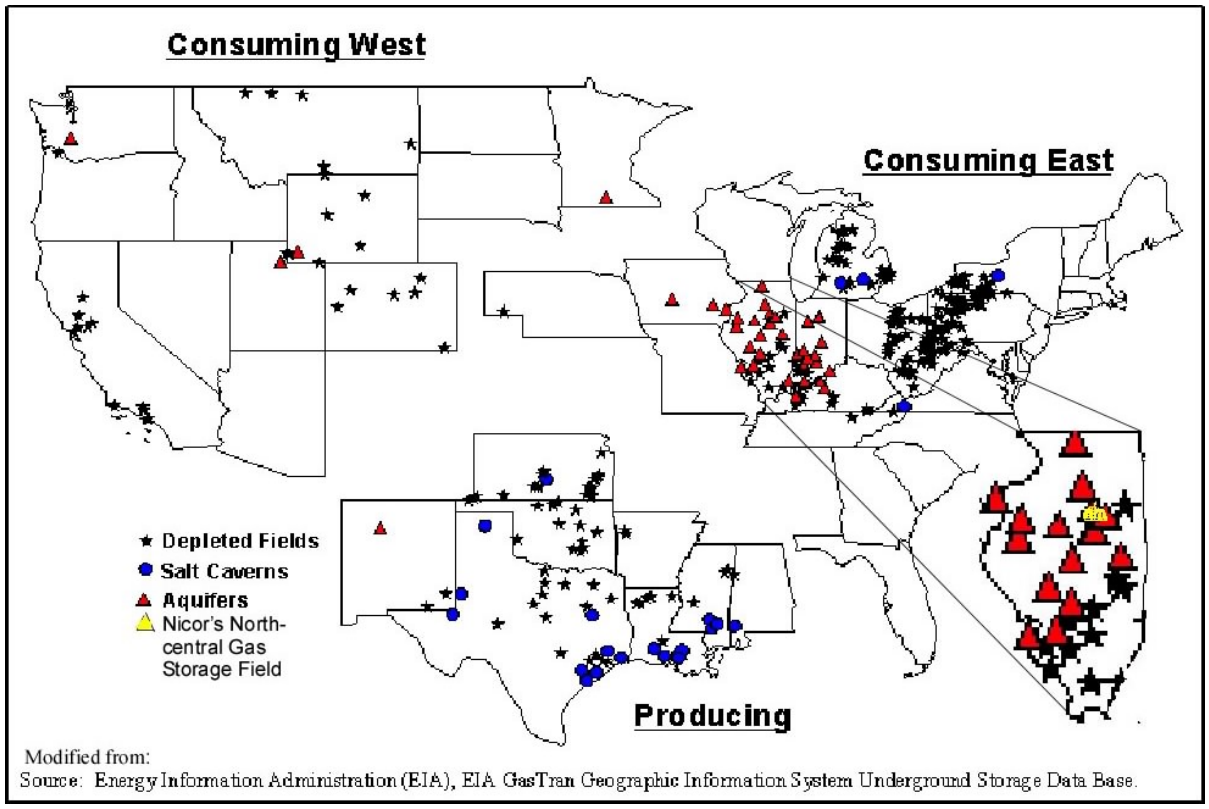

Figure 2: Underground Natural Gas Storage Facilities in the Lower 48 States, (modified from EIA, 2004).

Because the natural gas is stored in an aquifer, some gas mixes with the water.

Therefore, when the gas is withdrawn, it has to be separated from the water vapor. To dehydrate the methane, the methane is bubbled through triethylene glycol in a separator. Triethylene glycol is hydrophyllic. Thus, the water stays with the triethylene glycol, and the methane is released into an odorizer. After being odorized the gas is put on the market line where it will eventually be transported to homes and/or businesses. Even though water is being withdrawn from the reservoir, the quantity is insignificant when compared with the quantity of the natural gas being withdrawn. At the north-central Illinois field the quantity of water produced is so little that water wells to pump the water back into the reservoir are unnecessary (Katz and Coats, 1968).

If the volume of gas is not completely recovered every year during withdrawal, then the gas is being accumulated and/or dissolved. If the gas is accumulating, then it is building up in one or more of the formations within or above the reservoir. Additionally, if the gas is accumulating within formations above the reservoir, then the gas has to be migrating through the faults, drifting upwards due to a vertical permeability, or leaking due to mechanical problems within the wells. The gas could also be being pushed out of the side of the reservoir into a separate smaller dome (only in the case of overfilling of the reservoir). The gas may also be dissolved into the water on the edges of the reservoir. In this case, the gas bubble should be much larger than its current known size to accommodate 45 years of accumulation. However, when the observation wells were recently installed, insignificant, if any, amounts of gas were encountered during the drilling process. The data from the wells indicates the limits of the reservoir are not more than two to three miles from the underground gas storage main facilities in the north, west, and east directions (Harrigan and Lackie, 2003). No new wells were installed in the

southern edge of the reservoir; so whether there are significant amounts of gas in the ground water to the south is unknown.

According to the gravity survey and well logs, the east and north sides of the reservoir do not dip as sharply or as deep as the south and west sides. The east and north sides, the most probable directions to let gas escape from under the dome because of overfilling of the reservoir, are not leaking significantly. Another possible gas migration pathway is groundwater flow to the south through dissolution within the aquifer.

Furthermore, the gas is may be being captured within other formations in significant amounts, then it could be recovered for economic purposes by drilling wells to recover the gas.

Geologic and Hydrologic Setting

Stratigraphy and Sedimentology

The geology of the gas storage field area is dominated by Ordovician and Cambrian rocks that have undergone episodes of folding and faulting. Starting with the surficial material, the formations that exist within and above the reservoir are described in Figure 3.

The Ordovician formations consist of the Platteville Formation, St. Peter Sandstone, Shakopee Dolomite, New Richmond Sandstone, Oneota Dolomite, and the Gunter Sandstone (Figure 3). The Platteville Formation is a hard, dense, fine- to medium-crystalline dolomite. The St. Peter Sandstone is fine- to coarse-grained sandstone that is to some extent unconsolidated. The Platteville Group and the St. Peter

Sandstone exist throughout most of the field except in the southern portion of the dome structure (Plate 1). The Shakopee Dolomite is a micro- to fine-crystalline dolomite that has intermittent sandstone beds. The New Richmond Sandstone is fine- to coarse-grained sandstone that is unconsolidated in areas. The Oneota Dolomite is a micro- to medium-crystalline dolomite with a vuggy inter-crystalline porosity. The Gunter Sandstone in this area is a micro- to medium-crystalline dolomite with intermittent sandstone beds. However, excluding the storage area Gunter Sandstone is recorded as a sandstone and not dolomite.

The Cambrian formations include the Trempealeau Group, Franconia Sandstone, Ironton Sandstone, Galesville Sandstone, Eau Claire Formation, and the Mt. Simon Sandstone (Figure 3). The Trempealeau Group is a micro- to very fine-crystalline dolomite. The Franconia Sandstone is very fine- to fine-grained sandstone with argillaceous dolomite beds. The Ironton Sandstone is very fine- to coarse-grained sandstone with shaly dolomitic beds. The Galesville Sandstone is very fine- to coarse-grained sandstone with some unconsolidated areas and sporadic dolomitic beds.

The Eau Claire Formation and the Mt. Simon Sandstone are both used for gas storage and are split up into eight different units, the A Cap Rock, A Sand, B Cap Rock, B Sand, C Cap Rock, C Sand, Mt. Simon Cap Rock, and Mt. Simon Sandstone. The cap rocks consist of siltstone to sandstone with some dolomite and discontinuous shale beds; and the sands consist of sandstone with dolomite and shale inclusions.

Review of the well logs and literature has revealed possible depositional characteristics of a transgressive-regressive sea-level sequence. Well logs of the

Period	Formation or Group		Description
Quaternary	Wedron Group		Wisconsin age glacial till (~30 – 80 feet thick).
Ordovician	Platteville Formation		Dolomite fine to medium crystalline, hard, dense, vuggy, some fossil fragments with shale and chert inclusions (~0 – 120 feet thick).
	St. Peter Sandstone		Sandstone fine to coarse grained, partially unconsolidated and partially silicate cemented, well sorted, sub rounded to well rounded, clean (~0 – 180 feet thick).
	Shakopee Dolomite		Dolomite micro to fine crystalline, cherty, argillaceous, calcite growth with fractures, intermittent sandstone units with fine to coarse grains (~100 – 200 feet thick).
	New Richmond Sandstone		Sandstone fine to coarse grained, moderately to well rounded, sub-angular to well rounded, unconsolidated in areas, some dolomitic units (~80 – 100 feet thick).
	Oneota Dolomite		Dolomite micro to medium crystalline, hard, clean, chert veins, vuggy with intercrystalline porosity, sandstone units within, fine to coarse grained, sub-angular to rounded with dolomite cement (~120 – 160 feet thick).
	Gunter Sandstone		Dolomite micro to coarse crystalline, sandy to clean, hard, cherty, intermittent sandstone beds, fine to medium grained, angular to rounded, some unconsolidated (~100 – 130 feet thick).
Cambrian	Trempealeau Group		Dolomite with micro to very fine crystalline, hard to very hard, clean, some vugs and chert, partially glauconitic (~95 – 140 feet thick).
	Franconia Sandstone		Sandstone with very fine to fine grained, poor to moderately cemented, sub-angular to rounded, partially glauconitic with intermittent argillaceous dolomitic units (~120 – 140 feet thick).
	Ironton Sandstone		Sandstone very fine to coarse grained, rounded to sub-rounded, scattered unconsolidated grains, poorly to moderately sorted with intermittent very fine to fine crystalline argillaceous to shaly dolomitic units (~75 – 110 feet thick).
	Galesville Sandstone		Sandstone very fine to coarse grained, unconsolidated, well sorted, sub-rounded to well rounded with intermittent very fine to medium crystalline, dense, clean dolomitic units (~80 – 95 feet thick).
	Eau Claire Formation	A Cap Rock	Siltstone to sandstone, soft to firm, argillaceous, with mica, glauconitic and hematite stains, discontinuous shale beds and dolomite. Beginning of reservoir (~150 – 200 feet thick).
		A Sand	Sandstone, very fine to medium grained, sub-rounded to well rounded, well sorted to very well sorted, partially unconsolidated, very fine to fine crystalline dolomite cement, and granitic fragments (~60 – 70 feet thick).
		B Cap Rock	Siltstone and dolomite, very soft, very fine crystalline, dense, hard, with some laminar shale (~50 – 70 feet thick).
		B Sand	Sandstone very fine to medium grained, some scattered coarse grains and broken grains, sub-rounded to rounded, well sorted, shale inclusions, some unconsolidated beds (~50 – 60 feet thick).
		C Cap Rock	Dolomite, very fine crystalline, dense hard, clean to argillaceous (~30 – 40 feet thick).
		C Sand	Sandstone, very fine to coarse grained, pure silicate cement, sub-angular to sub-rounded, poorly sorted, shale and fossil inclusions, dolomite fragments (~30 – 40 feet thick).
		Mt. Simon Cap Rock	Siltstone, firm to hard, slightly dolomitic, some sandstone, fine to coarse grained, some shale inclusions (~20 – 30 feet thick).
	Mt. Simon Sandstone		Sandstone rounded to sub angular grains, moderately to poorly sorted, very fine to very coarse grained with soft to firm discontinuous shale units. Also, used for gas storage (~2000 feet thick).

Figure 3: Stratigraphic Column of an Underground Gas Storage Field in North-Central Illinois (Harrigan and Lackie, 2003; Willman et al., 1975)

reservoir, Eau Claire Formation and Mt. Simon Sandstone, show the lithology of the Eau Claire Formation grading from siltstone in the uppermost portion of the Eau Claire Formation to sandstone and back and forth until the Mt. Simon Sandstone which is a sandstone. This is indicative of a transgressive-regressive sea level sequence of the Illinois Basin. Also, the Mt. Simon is the thickest in Illinois to the east of the field towards Chicago, Illinois. The basin is known to be to the throughout Illinois during the Cambrian. Also, the Eau Claire Formation grades to sandstone to the north and west in Illinois and to dolomite to the east and central Illinois from the Chicago, Illinois area (Willman et al., 1975). Also, there is evidence of fossils and intermittent dolomitic beds and shales (Figure 3) (Willman, et al., 1975).

The A sand of the Eau Claire Formation and the Mt. Simon Sandstone are indirectly connected because of the faulting. Accordingly, the reservoir has been divided into zones. They are the A sand North, the A sand South, the B sand North, the B sand South, the C sand North, the C sand South, the Mt. Simon Sandstone North, and the Mt. Simon Sandstone South. Each is used for gas storage and has a corresponding cap rock.

Structural Geology

The underground gas storage field is a small dome shaped structure, with a total surficial area of less than 20 square miles, within the northern segment of the LaSalle Anticlinorium. The LaSalle Anticlinorium developed during the Late Paleozoic (McGinnis, et al., 1976; Nelson, 1995).

The western portion of the dome, a part of the Peru Monocline, has about 1,500 feet of relief. The other portions of the dome dip more gently. The LaSalle Anticlinorium

extends from Lee to Lawrence Counties in Illinois. Not much is known about the deeper structure of the LaSalle Anticlinorium, in part because of the lack of publishing done in the oil and gas industry. However, many sub-parallel anticlines, domes, monoclines, and synclines exist. The majority of the folds within the LaSalle Anticlinorium are positioned north-northwest strike of the larger structure. The Peru Monocline is the northernmost major fold of the LaSalle Anticlinorium. The Peru Monocline, like the other folds, is topped by irregular domes, such as the one in question. Most of the uplift of the LaSalle Anticlinorium occurred in the Late Paleozoic Era. Roughly half of the uplift took place before Pennsylvanian sedimentation and after the Chesterian. The result is an angular unconformity in which Ordovician rocks are overlain with Pennsylvanian in the northern segment of the LaSalle Anticlinorium which is outside the storage reservoir area. During the Middle Pennsylvanian uplift is evident by thinning of a number of beds and intervals. Following the Pennsylvanian, major folding continued (Nelson, 1995).

Subsequently, the storage field is faulted, fractured, and jointed immensely with many fault zones; one zone is differentiated from the others in the southwest corner of the field (Plate 2). There is one major fault within the gas storage field with a displacement of approximately 150 feet (Plates 1 and 2). The displacement on the fault is such that on the north side a quarry is mining the Platteville Formation, and on the south side other quarries have mined and are still mining the St. Peter Sandstone. The estimated displacement is 60 – 150 feet. Within the underground gas storage field, the St. Peter Sandstone is completely missing throughout the southern gathering system (the top of the dome to the south of the fault). At the top of the dome in the southern portion of the field, the Shakopee Formation is just below the Wedron Group. Recently, gas migration

in the southern portion of the field may suggest that there are more faults or fractures and jointing than what was previously thought (Nelson, 1995). On the south side of the field, the Platteville Formation has been eroded away, but is still existent throughout the northern portion of the field.

Hydrogeology

Groundwater flow is mostly to the east, with some flow in the south and west directions within the Mt. Simon Sandstone and the Eau Claire Formation (Bond, 1972). The four units used for gas storage have sufficient porosity and permeability, as evidenced by recordings by the oil and gas industry. However, porosity and permeability of shales and siltstones were not recorded as they are not useful in production. Porosities for the Mt. Simon Sandstone range between 10 and 15%. Porosities for the Eau Claire Formation range between 17 and 18.6%. Permeabilities for the Mt. Simon Sandstone range between 15 and 185 millidarcies. Permeabilities for the Eau Claire Formation range between 150 and 556 millidarcies. It should also be noted that many of these values are from areas identified as anticlinal structures or bedrock domes (Buschbach and Bond, 1973).

The Eau Claire Formation cap rock of siltstone is about 150 to 200 feet thick. Logs taken during the placement of the newest observation wells have shown evidence of unconsolidated materials within the reservoir sands and unusually high porosities within the reservoir cap rocks. This suggests that a secondary porosity was developed during the formation of the LaSalle Anticlinorium.

Within the area, there is a lack of any high producing water wells that create a large drawdown in the area. The area contains residential wells, and at no time were any

large irrigation activities observed in the area. The closest well in the area that would have a large drawdown is about seven miles south of the gas storage field and is within the Galesville, Eau Claire Formation, or Mt. Simon Sandstone.

Previous Work

Over the last 45 years the pressure within the aquifer has been monitored and recorded. At first, readings were taken only three times a week from one well, but now the pressure is monitored on a daily basis in fourteen wells. Eight wells were chosen for reservoir pressures each from a zone, and another six wells are used in gauging the flow pressures. Over the years the designated wells have changed, but only within their respective zones. Moreover, pressure data are digitized in some cases and saved for future use (Deters, et al., 2003).

To control a surficial gas show, the pressure in the A Sand has been reduced. Pressures in the A Sand have been reduced to well below the aquifer equilibrium (kept at or below 570 bhpsia). This helps to control gas migration to the surface and reduces the amount of gas within the vadose zone decreasing crop damage. Of course, the surficial gas spot could be a product of a small hole in the side of an A Sand well near the surface and near the gas spot. However, it could also be the product of vertical migration through the bedrock from the reservoir.

Gamma ray - neutron logs have been run periodically on many wells throughout the storage field. As a result, all 120 wells in the reservoir have gamma ray – neutron logs, but only about fifty have digitized logs, digital copies readable by well log analysis software.

Gas saturation is apparent in the well logs in other units of the reservoir even though those units are not being directly injected into near that particular point. For instance, the P. Mathesius 17 (Figure 4-PM 17), an observation well in the C Sand of the inter-fault zone, shows gas saturation in the A Sand. The well is perforated in the C Sand only, and there are other wells that are withdrawing all year in the A Sand inter-fault zone.

Gravity surveys were conducted over the reservoir during its development. They show the general topographic relief of the formations in all four directions. Because some of the original gravity survey is missing, the gravity surveys cannot be used for more than general purposes.

In the Midwest, gas storage fields are monitored for mechanical problems by frequently running gamma ray – neutron logs of various wells within the gas storage field. Some other techniques for monitoring gas storage fields are time lapse seismic and high resolution 2D and 3D seismic methods, use of geochemical markers, and transient electromagnetics (Nissen et al., 2004; Medeiros and Bicego, 2004; Ziolkowski et al., 2002; Vidal et al., 2002; Dumont et al., 2001; Blondin and Mari, 1986). Time lapse seismic or 4D seismic monitoring is used to monitor the movement of the gas bubble within a gas storage field. Time lapse seismic detects the changes in fluid and rock properties such as density, velocity, pressure, and temperature. The Cere-la-Ronde underground gas storage field has many of the same geologic characteristics as Nicor's gas storage field. The gas storage field is within a sandstone aquifer in a faulted anticlinal structure within the Paris Basin southwest of Paris, France. Geomechanical modeling was used to bring time lapse seismic data, well log data, and other reservoir

information together to form a better picture of the reservoir. The work found that calibration of well logs and the seismic survey are essential to gas saturation interpretation (Vidal et al., 2002).

High resolution seismic detection has been used to delineate gas migration from a reservoir. Nissen et al. (2004) found that gas was in the formations above the reservoir at the Yaggy Gas Storage Field in Hutchinson, Kansas. The Yaggy Gas Storage Field is gas storage within salt caverns. The gas that had migrated was primarily found in the fractures. Pockets of gas were found to cause a bright spot on the p-wave profile that was unique from any other formation anomalies.

At the Gaz de France underground gas storage field near Gournay-Sur-Aronde about 80 km northeast of Paris, France, gas saturation is measured with neutron logs, and the gas bubble boundary migration is measured with high resolution seismic. The gas is stored in an anticlinal structure with two domes and a northwest orientation. Research discovered that the gas preferentially migrated to the southeastern limb of the anticline. The gas was also migrating towards the northwest limb of the anticline within the reservoir (Blondin and Mari, 1986).

Statement of the Problem

At this gas storage field gas is present at the surface causing the retardation of crop growth at one location spot within the southern portion of the field. Previous work has indicated that the crop damage is closely related to the pressures within the A Sand of the Eau Claire Formation. When the pressures are below 570 bhpsia in the A Sand of the Eau Claire, the crop damage is kept to a minimum. However, at higher pressures the gas

within the pore space at the surface exterminates all plant life in the area with the most gas (Deters et al., 2003 and personal observation). How the gas is being transmitted to this location and whether it exists anywhere else near the surface is the purpose of this study. Possible migration pathways include geologic causes or mechanical problems such as leaks within wells. The objectives are as follows:

- Use a volume of shale evaluation to determine whether possible pathways within the reservoir due lithological variability and structural deformation.
- Calculate average porosity and standard deviation for each unit to delineate possible vertical pathways.
- Identify shallow faults capable of conveying the gas to the surface.
- Identify where gas is present within the surficial deposits and shallow bedrock using a high-resolution shallow seismic survey.

Shale Volume

Major gas flow within the reservoir is apparent, in and out of the wells. Other types of gas flow within the reservoir could include possible conduits within the well casings, flow along the faults, and interaction with the aquifer fluids through dissolution. Questions exist about the true nature and shale content of cap units within the storage field. Aside from the Eau Claire Formation and the Shakopee Formation, which comprise the surficial bedrock in the southwest corner of the field, there seems to be a lack of a cap rock to capture gas migrating upwards which is the surficial bedrock in the southwest corner of the field (Plate 1). Shale volume calculations will be used to verify the integrity of the cap rocks and to identify possible vertical pathways to the surface.

Other investigators have found that shale volumes are useful in the calibration of well logs (Dresser, 1982). Gamma ray logs are used to obtain formation density from within the borehole. Once calibrated to well-logs, the differing densities indicate the amount of shale that is present (Dake, 1978).

Porosity

Three new observation wells were recently drilled along the edges of the storage field. Formation porosities within and above the reservoir will be obtained from porosity logs acquired post drilling.

The bulk density porosity (porosity derived from bulk density logs) from the latest wells that were drilled will be the best estimate of the porosity for all the formations that are within and above the reservoir (Mills, et al., 1991). Gamma ray – neutron logs have been taken throughout the field. However, the presence of the gas has skewed the neutron counts and therefore neutron porosity would not be as accurate. Determination of the porosity will help in determining whether the gas has a possible pathway upwards through the various formations, which may reaffirm or contradict the shale volume data.

High-Resolution Shallow Seismic Survey

A high-resolution shallow seismic survey was performed and analyzed to determine the existence of gas near the surface and to gain a better understanding of the near-surface bedrock. Vidal et al. (2000) found that well log analysis was very useful in the validation of seismic surveys. Using the newly acquired seismic data, an improved

picture of the bedrock was attained along with a greater knowledge of the structure and sedimentology.

CHAPTER II

SHALE VOLUMES

Methods/Materials

Volume of shale (V_{sh}) was evaluated to determine the amount of heterogeneity within each unit. The V_{sh} measurement is actually a grain size analysis. The V_{sh} is a record of the natural gamma rays that come from thorium and potassium in shales or clays (Fertl and Chilingarian, 1990). Log analysis was employed to determine the V_{sh} within every sandstone unit and within the cap rocks for each unit of the reservoir. Using the linear V_{sh} calculations the gamma ray curve is quantified into a percentage. The highest gamma ray value is equal to 1 or 100 percent, while the lowest value, zero, which is the response to sand or larger grained material. Less clay or shale is represented by more quartz or calcite crystals and therefore less natural gamma rays (Dresser Atlas, 1982).

The V_{sh} was calculated using gamma ray logs of 29 wells throughout the field (Figure 4). The wells were picked based on the availability of digitized logs and geographic location. Digitized logs are available for the wells that have been logged in the last ten years.

The V_{sh} was determined by changing the numerical value of the gamma ray log to a percentage (an arithmetic value so 100% is 1.0 and 50% is 0.5). The equation used was:

$$V_{sh} = (\gamma_{log} - \gamma_{cln}) / (\gamma_{max} - \gamma_{cln})$$

where γ_{log} is the gamma ray value at a depth, the γ_{cln} is the minimum value on the specific well log, and γ_{max} is the maximum value on the specific well log (Dresser Atlas, 1982). All of the units were determined by a major change in grain size, when the percentage of shale dropped below or went above 50%. After the calculation for $V_{sh,}$ the total average of each unit was determined and a standard deviation was produced. The calculated V_{sh} values were mapped showing the V_{sh} distribution using Surfer 8 software to determine heterogeneity or consistency of grain size within each of the units (Figure 5).

Wells that were analyzed and the calculations are listed in Table 1 in the Appendix. The Vsh Distributions are represented in Figure 5.

Due to a lack of correlation between gamma ray logs that were taken before API units were used and the present, a change in the volume since the beginning of the reservoir cannot be calculated. API units are the industry standard unit for measuring gamma rays. All of the tools used to log wells are standardized to a specific test pit. This way logs can be compared to each other. There is no way to calibrate instruments to each other completely. However, by calculating a minimum and maximum for each log and then using those numbers to adjust the log, one can compare the logs to each other (Dresser, 1982). Each gamma ray – neutron-logging machine is calibrated to an international standard and is slightly varied day to day which causes a certain amount of error. The amount of error is never truly known because well logs are the most inexpensive way to gauge the properties of the reservoir. It can only be assumed that as time goes on the quality of the well logs improves because there are less anomalies that are found when production starts. However, well logs have just been calibrated to what

is assumed a normal value and every well log is run off the one standard. In addition, variability from day to day of the nuclear sources for the tools that are used causes changes in the well logs.

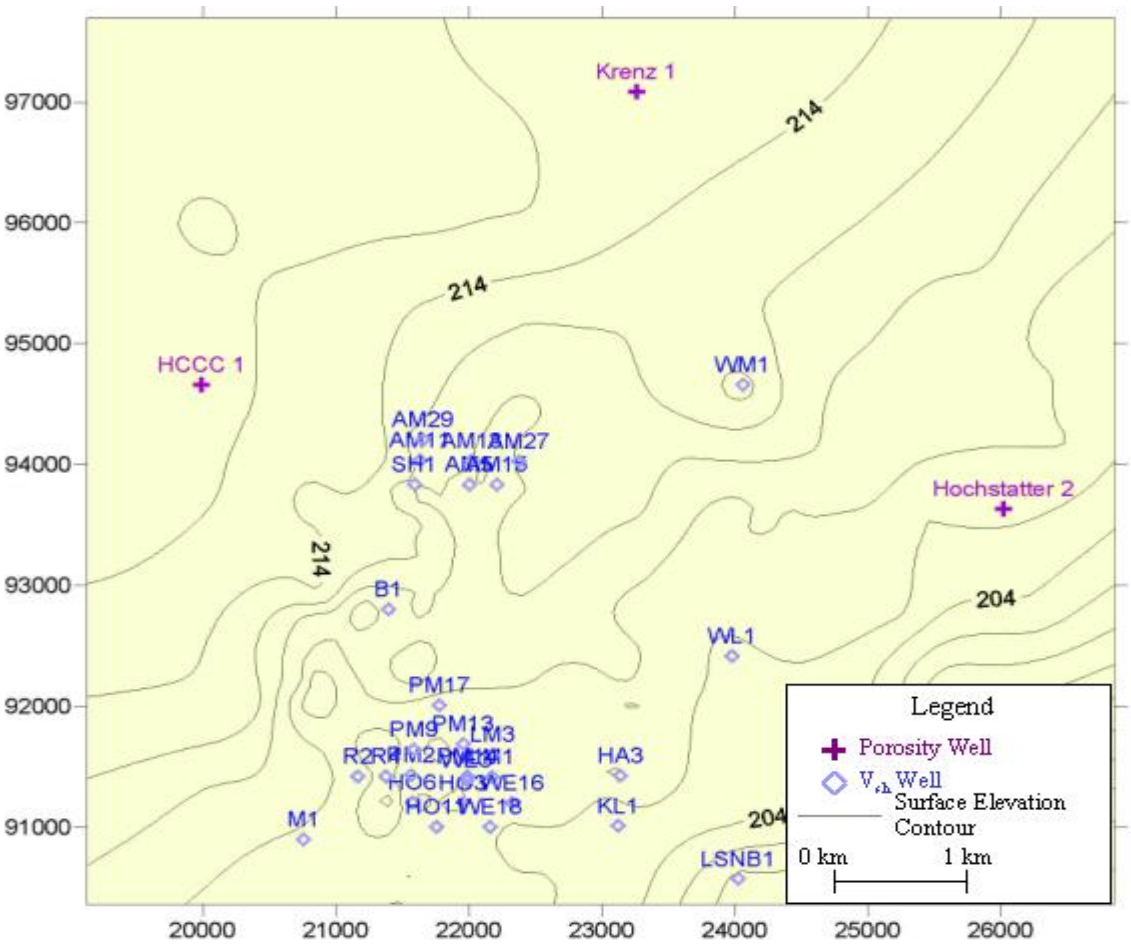

Figure 4: Vsh and Porosity Well Locations

Results

The distributions of Vsh values were found to be heterogeneous; especially in the

north and south gathering systems. This is most likely a result of a lack of data everywhere else in the field, since the main concentration of wells is in the gathering system (Figure 4). Where the most data is present is also where the most heterogeneity appears on the Vsh Distribution maps (Figure 5).

The data indicate that the Eau Claire Formation Cap Rock of the reservoir is a siltstone, which is in agreement with results of the mud logger, and that nowhere throughout the reservoir does it grade to shale in a large enough amounts to be evident within the averages for each well. The A Cap Rock is heterogeneous and may be less of a cap rock than previously thought. Additionally, a low in the volume of shale distribution appears throughout the different units almost directly in line with each other, as highlighted by red boxes in Figure 5. Each cap rock has a seemingly deeper low, but this is due to the fact that the sandstones are already fairly low in their volume of shale content. The standard deviation for each unit is shown on Table 1 (See Appendix).

The sandstones varied from low 40s to less then 10%, but the standard deviation for each unit excluding the B Sand shows that the sandstones were less heterogeneous than the cap rocks (Table 1 – Appendix B). The cap rocks varied from mid 80s to low 40s and were more heterogenous within each unit. The B Cap Rock was the most homogeneous cap rock.

A great deal of heterogeneity exists within each unit; however, the most alarming is the Eau Claire Formation A Cap Rock. Being the uppermost unit, homogeneity and a solid higher volume of shale is needed. However, the unit exhibits the same characteristics that each subsequent unit does, having a low depression in both the north and the south gathering systems. The depression in the north is not surrounded by as

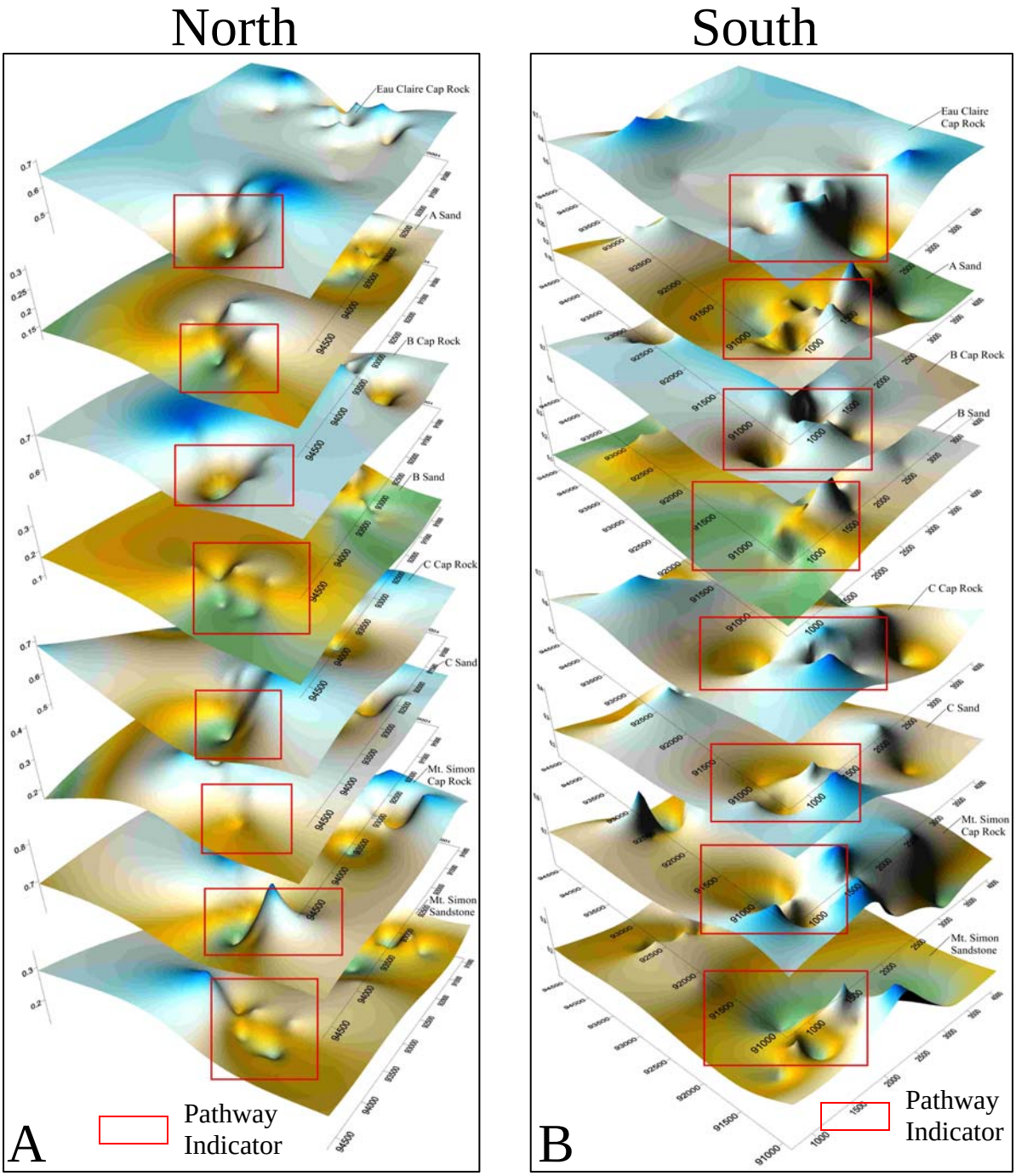

Figure 5: V_{sh} Distribution, depressions indicate areas of lower shale content; A shows the possible migration pathways in the north side of the field; B shows the possible migration pathways in the south side of the field.

much heterogeneity as in the south. This may be a product of less data; there are more wells in the south than there are in the north. This is in part because the south portion of the field was developed first and only later after several faults were discovered the north gathering system was developed.

The wells used for this study seem to be clustered in the center of the reservoir area; this is because the majority of the gas is also stored year around in the center of the reservoir area. Better knowledge is needed for this center area, as the gas is most likely to migrate upwards in an area that it is constantly present. The gas is always in flux, but due to flow patterns the gas may have drifted into areas that are not in the direct flow path of the wells causing it to be more likely to drift upwards.

The A Sand of the Eau Claire Formation seems to be the most homogeneous of the four units used for gas storage, but is not the best unit for gas storage. The B Sand of the Eau Claire Formation was found to have the least amount of shale. The C sand of the Eau Claire Formation has the most shale within it and in most cases it is very hard to discern an actual unit. The C Sand is the most heterogeneous of the four units. The Mt. Simon Sandstone is not the best or the worst and has about four percent more shale within it than the A Sand on average.

Not only are the Eau Claire Formation and Mt. Simon Sandstone heterogeneous having members that vary from limestone to shale to sandstone, but each member is heterogeneous within itself.

The Mt. Simon Sandstone has less shale as a formation than the Eau Claire Formation. Comparison of the Mt. Simon Sandstone shale volumes to the Eau Claire

Formation shale volumes will help determine which formation is best for gas storage. A large amount of discontinuous shale beds within the C Sand and the Mt. Simon Sandstone units inhibits flow of the natural gas. Even though a majority of the natural gas at Troy Grove is being stored in the Eau Claire Formation, mainly the B sand, the majority of the natural gas is being injected into the Mt. Simon Sandstone. Other than migration due to the faults, the shale volumes may influence migration and accumulation of the natural gas within the Eau Claire Formation. Also, in coordination with structural data shale volumes may help determine areas in which the gas is more likely to migrate upwards due to a lack of shale.

Discussion

The known gas migration within the reservoir supports the V_{sh} results. Nicor has found that even though most of the gas is injected into the reservoir through the Mt. Simon Sandstone, eventually only about five percent of the total amount of natural gas within the reservoir is stored in the Mt. Simon Sandstone (Deters et al., 2003). The Mt. Simon Sandstone was originally intended to be the only formation used for gas storage. Now, the Eau Claire A, B, and C Sands are used for storage with siltstone units dividing each.

There is a great amount of heterogeneity within each unit indicating that the reservoir may be highly unpredictable. Discontinuous shale beds are irregularly intermingled within both the sandstone and siltstone beds. The standard deviation of the average shale volume for each unit is between .0498 and .0749 (See Appendix).

The A Cap Rock is heterogeneous between wells that are fairly closely spaced (within 100 feet). The A Cap Rock is a siltstone with varying amounts of clay. The uppermost 50 -100 feet contain clearly less clay material than the underlying portion of the A Cap Rock. In the north portion of the field the wells vary from 41.7% to 70.7%. The minimum and maximums were both found in wells that were within the main cluster of wells which excludes the Whitmore 1, Whitlock 1, and Becker 1. In the south portion of the field the minimum and maximum are 40.2% to 71.3%. However, the 71.3% comes from a well outside of the main cluster, Klinefelter 1. Within the main cluster of wells there is a maximum of 69.5%, Hoffman 6. Again the heterogeneity increases with the amount of data points. Because the Surface Distributions were krigged, they exhibit more heterogeneity where there are more data points (Figure 5). This also reveals the possible preferential pathways of vertical gas migration, as shown by the red squares in Figure 5.

It should be pointed out that the A Sand, B Sand, C Sand, and Mt. Simon Sandstone communicate due to the displacement of the fault and the many fault zones. The main fault has a displacement of 150 feet, so the Mt. Simon Sandstone is in direct communication with the B Sand. Likewise, the A Sand is in direct communication with the Eau Claire Cap Rock and possibly the Galesville Sandstone in some portions of the dome structure.

The C Cap Rock and the C Sand could be classified as the same unit, if it were not for the amount of gas being stored there. The logs indicate that the C Sand is very shaley, although in some areas not as much as others. It is the inconsistency of the shale beds throughout the unit that allows for gas to be stored. Discontinuous shale beds exist

throughout each unit, but because each is discontinuous they do not serve as a cap, just a minor divider between layers within the same unit in a specific spot.

All of the other units have high variability in the location of the discontinuous shale beds and amount of discontinuous shale beds. Also, the B Sand has areas that are greater than 25% shale. The unit has a considerably large layer of siltstone and shale in the middle of it, but is consistently sandstone otherwise (See Appendix).

Interestingly, the Eau Claire Formation is supposed to be 450 feet thick of sandstone and shale alternating. Looking at the evaluations in Table 1 and Figure 3, it is evident that the Eau Claire Formation was almost never a shale, and alternates between siltstone and sandstone.

The heterogeneity of the Eau Claire Formation and the Mt. Simon Sandstone confirms that the area has been greatly modified by structural deformation. Variability in Vsh among wells within such close range of each other is not due to depositional processes alone.

Comparing the Vsh illustrates the variability of the units within the field. Variability exists within individual units and among the various units within the field. The heterogeneity reveals a more complex geology than originally believed. This complex geology suggests that gas may migrate vertically towards the surface along areas with low Vsh. More detailed investigation into the stratigraphy and structure are needed to completely understand the reservoir. More wells need to be analyzed and better structural data needs to be acquired.

In Figure 5, the areas highlighted by the red squares imply a similar vertical permeability. The lack of material with impermeable qualities is clear both in the north

and the south. The irregular pattern of the heterogeneity also indicates that structural deformation has occurred.

CHAPTER III

POROSITIES

Methods/Materials

The porosity of every formation from the surficial bedrock to the bottom of the reservoir needs to be calculated to determine whether it is possible that gas migration is occurring through the cap rock and overlying units vertically due to the existence of fault zones, especially along the major fault that runs East – West through the reservoir and overlying formations. Using the well logs for Krenz 1, HCCC 1 and Hochstatter 2, a porosity curve was calculated for each formation and adjusted for formation properties and drilling mud. The digitized logs provided data for every one quarter of a foot or half of a foot. The porosity curve was produced from the density logs taken from the open hole before casing was installed.

The three wells being used are just outside the gas storage field, but are close enough in proximity to share many of the structural and hydrologic properties. The HCCC 1, extends to the Mt. Simon Sandstone, has significant gaps in the log data, so the porosity curve was incomplete for a large portion of the Eau Claire Formation Cap Rock. However, the absence of data did not significantly skew the findings.

Results

In Table 2 and Figure 6 the individual porosities for each unit and well are shown along with the standard deviation. There does not seem to be any pattern such as one well having higher overall porosities. The porosities for each unit are variable. There is a need for more data. However, the Eau Claire Cap Rock, a siltstone, has an unusually high porosity. Within the individual logs, porosities were as high as 56% and as low as 3 or 4 %. However, most of the unit was above 15% in each of the logs. This could be indicative of a secondary porosity.

Discussion

Oil and gas companies that are using the formations for storage or production report porosity data for various formations. Likewise, only porosities for units that are used for storage or production have been reported. In Illinois porosities for the St. Peter Sandstone, Galesville Sandstone, Eau Claire Formation, and the Mt. Simon Sandstone have been reported. The St. Peter Sandstone varies from 14 – 18%. The Galesville Sandstone varies between 15.2 and 18%. The Eau Claire Formation is fairly steady at 17 and 18.6%, one of which is from the same area as the reservoir. The Mt. Simon Sandstone varies between 10 and 15%. As for the many other formations studied no porosity data was available. Also, it should be noted that the porosity data is from areas that have undergone structural deformation at some point. Some are dome structures and others have been identified as anticlines (Buschbach and Bond, 1973).

The St. Peter Sandstone within the reservoir area has a porosity of 24.7 – 27.6%. This is much higher than the reported values, which indicate a secondary porosity. The

Galesville Sandstone is much higher and more variable at the reservoir area. The porosities vary between 23.5 and 56.3%. The Eau Claire Formation sandstones vary between 15.2 and 19.0% in the C Sand, 18.6 and 20.4% in the B Sand, and 19.8 and 23.2% in the A Sand. The A and B Sands are a little high compared with the values reported. The Mt. Simon Sandstone varies from 19.1 – 22.3%, which is high when compared to the reported values.

As far as the other units within the reservoir go, including the Mt. Simon Sandstone, A Sand, B Cap, B Sand, C Cap, and C Sand, the sandstones are high porosity sandstones which were already known. The siltstones have porosities that are much lower than the cap rock and not suggestive of a secondary porosity.

The Franconia, Ironton, and Galesville Sandstones are fairly high porosity which was to be expected. However, the Krenz 1 porosities showed porosities around 56% for the Galesville, 46% for the Ironton Sandstone, and 43% for the Franconia Sandstone unlike the other two wells (Table 2). This may signify significant structural deformation in the north portion of the field. Also, higher porosity may indicate a possible storage mechanism causing less gas to migrate to the surface.

As far as most of the other formations go, there are not any huge anomalies between any of the wells. The sandstones are high porosity ranging from 19% to 28%, and the dolomites are fairly low porosity ranging from 6% to 13%.

Table 2: Porosity Data for the HCCC 1, Krenz 1, and Hochstatter 2; porosity values are average for each formation.

Formation	Krenz 1	Hochstatter 2	HCCC 1	Stand. Dev. 3 Wells	St. Dev. K1	St. Dev. H2	St. Dev. H1
Platteville	7.27	12.90	6.38	3.53	8.99	10.25	4.08
St. Peter	26.22	27.62	24.70	1.46	4.29	3.40	9.53
Skakopee	7.72	8.75	8.06	0.53	5.42	4.16	4.47
New Richmond	20.35	22.77	18.66	2.06	6.17	5.73	7.44
Oneota	8.21	10.52	9.41	1.15	4.91	5.55	4.76
Gunter	5.65	7.93	8.19	1.40	5.72	5.31	6.12
Trempealeau	6.09	8.03	6.47	1.02	4.80	5.43	5.03
Franconia	43.48	17.54	17.03	15.13	5.99	5.48	4.09
Ironton	45.95	19.64	14.14	17.00	8.22	5.49	4.94
Galesville	56.29	25.46	23.54	18.38	8.78	5.24	2.92
Eau Claire Cap	25.60	21.28	20.41	2.78	10.33	5.78	7.92
A Sand	19.82	23.17	20.44	1.78	2.83	1.58	3.51
B Cap	5.59	10.52	8.63	2.49	5.36	4.14	4.70
B Sand	19.74	20.39	18.63	0.89	4.10	3.49	2.93
C Cap	6.16	11.54	12.38	3.38	4.22	3.58	6.56
C Sand	15.16	18.95	16.85	1.90	3.17	5.59	4.65
Mt. Simon Cap	10.73	14.37	13.48	1.90	2.87	1.88	2.39
Mt. Simon Sand	19.11	22.32	20.28	1.63	2.79	2.95	2.77

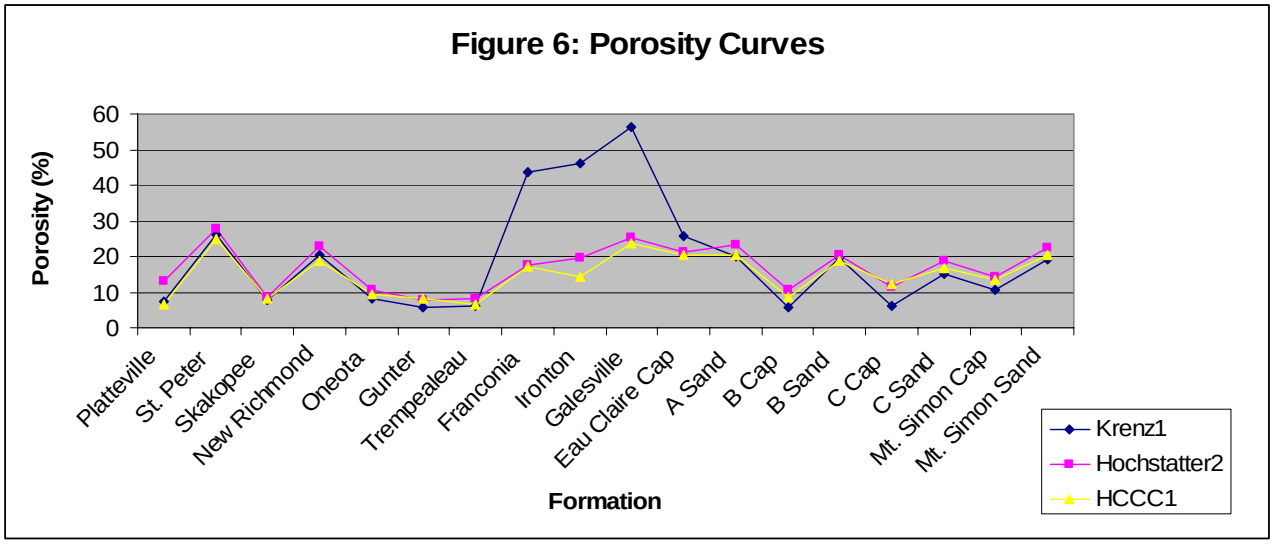
Figure 6: Porosity Curves
Porosity (%)
60
50
40
30
20
10
0
Platteville
St. Peter
Skakopee
New Richmond
Oneota
Gunter
Trempealeau
Franconia
Ironton
Galesville
Eau Claire Cap
A Sand
B Cap
B Sand
C Cap
C Sand
Mt. Simon Cap
Mt. Simon Sand
Formation
Krenz1
Hochstatter2
HCCC1

CHAPTER IV

SEISMIC SURVEY

Methods/Materials

Shallow P-wave and SH-wave seismic reflection were used to delineate the existence of gas within surficial sediments and shallow bedrock, including the Platteville Formation, St. Peter Sandstone, Shakopee Dolomite, and New Richmond Sandstone, and to determine the amount of structural deformation within the shallow bedrock. SH-wave and P-wave seismic reflection are both based on the calculation of the travel time of acoustic waves in layered media. Seismic velocity and bulk density of the rock units are the key properties that control sound propagation through the media. Figure 7 exhibits a seismic pulse (sound wave) traveling through the ground and being reflected as it encounters a differing rock unit. This reflection is a result of an impedance contrast when the combined contrast of unit velocities and densities change. Both the P-wave and SH-wave geophysical methods had a controlled energy source to impart sound energy into the ground and very sensitive receivers, geophones, to identify the sound as it returned to the surface by refraction or reflection. Refraction is when the sound pathway is changed, refracted beneath the surface which can occur both vertically and horizontally. During this study the SH-wave data was collected from horizontally refracted sound waves (Pugin, 2005).

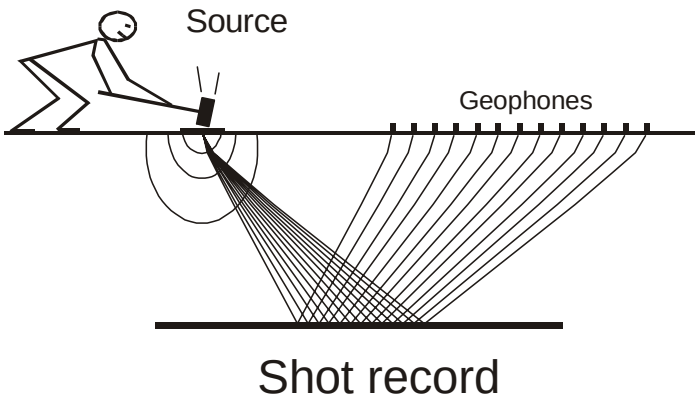

Figure 7. Ray path of a sound pulse traveling into the ground and being reflected at an interface (Pugin, 2005)

P-wave seismic reflection was used primarily to determine where gas was present near the surface. P-wave refraction can be used, but most likely would not have yielded results that were as satisfactory. Changes associated with density do not have as strong of a signal in all material types and therefore P-wave refraction is not as reliable (Pugin, 2005).

Quantification of the gas was not possible with the available techniques. Very small amounts of gas cause very strong impedance contrasts. In turn, the seismic survey was successful in determining whether gas was present, but not specific quantities. Boreholes in areas where the P-wave survey indicated that gas was present could be used to determine the amount of gas that is present in the subsurface, but so far this has not occurred (Pugin, 2005).

In Figure 8 two P-wave seismic shot records are shown. Figure 8A shows quality data with little interference; and Figure 8B shows data that has been absorbed due to very shallow gas reflections (Pugin, 2005).

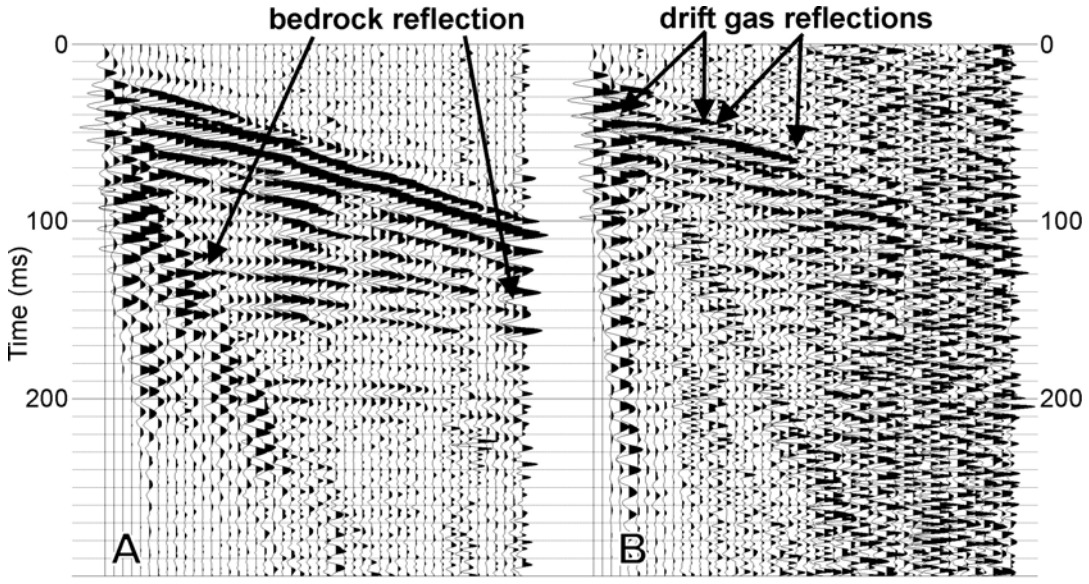

Figure 8: Two P-wave seismic shot records showing A. good quality data B. poor quality data due to high absorption with very shallow gas reflections (Pugin, 2005).

SH-wave seismic refraction was used to determine soil and rock properties such as formation changes, structural deformation, and lithological changes. SH-wave seismic refraction is not impeded by porosity content. However, SH-wave seismic refraction will be absorbed if it encounters fluids or gases. If there are conduits within the rock or soil, there will not be any data for that area. In turn the structural deformation and formation and lithological changes were for the most part well defined.

The seismic survey was performed during the summer of 2004. The survey reached a depth of a few hundred feet, intersecting the surficial bedrock. North-south and east-west two-dimensional seismic profiles, primary wave and secondary wave, were shot. The profile lines were chosen to intersect all of the known faults and to reveal the dip component at the surface of the bedrock. The SH-wave profile was shot throughout most of the field (Plates 1 and 2). The P-wave profile was shot in selected portions of the field, but north-south and east-west profiles were attained. The data were collected with

vibroseis™ technology. The data were interpreted and used to determine where the shallow gas was located and to identify any pathways that gas may travel near the surface. The shallow seismic survey data was interpreted with the use of Seismic Micro-Tech 2d/3dPAK.

Only wells that were along roads where the seismic survey was taken were used in the interpretation. The majority of the wells within the gas storage field were positioned together in a rectangular pattern in the north and south portions of the field. This is where the domes in the north and south portions of the field are the highest and the gathering systems are in place for gas storage (Figure 4). Also, structure test wells installed and logged during the development of the field were used for interpretation. However, only formation tops were available for the structure test wells. All digitized gamma ray – neutron well logs that were available were entered for interpretation. There are no existing acoustic logs for this particular field, so ground truthing of the time-depth intervals for the various formations will have to be done at a later date. The gamma ray – neutron logs were attained only from wells that are observation or injection withdrawal wells still in use now or that have been in use within the last 15 years. Additionally, depth to formation tops was entered for use during interpretation. All wells that had formation top data and that were along the roads used in the survey were used.

Data Acquisition and Processing

The seismic survey of both the SH-wave and P-wave took a total of seven weeks, two weeks for the P-wave and five weeks for the SH-wave. During this time about 24 miles of seismic profiles were recorded (Plates 1 and 2).

Landstreamer technology, known to be comparable to geophones planted into the ground, was used in the acquisition of the seismic survey. Because landstreamers were used, all data acquisition occurred on roads, gravel or pavement, and not on grass or soil, which can cause interference. The landstreamer for the P-wave survey had 24 geophones on sleds spaced at 3m and towed behind a vehicle (Figure 9). The energy source is from a weight dropper with a 100- or 30-lb hammer that is mounted on a trailer (Figure 9). All the data acquisition characteristics for both the P-wave and the SH-wave are in Table 5 (Pugin, 2005).

For the SH-wave 12 geophones on sleds were used to record the seismic data. Unlike the P-wave, a hand held sledge hammer was used to hit a metal plate three times for each shot (Figure 10). A horizontal shear wave was propagated by the three successive hits to the metal plate. Also the sledge hammer sent a signal to the geophones to cause them to record every time the metal plate was hit. For both the SH-wave and the P-wave, GPS was used to record the location of the shots when they were taken (Pugin, 2005).

P-wave processing started with viewing and picking the actual primary wave from the raw data (Figure 8). In most cases, there were a lot of noise and background interference with the data. Once the primary wave was picked the data were filtered to remove the noise. After filtering, the P-wave data went through a muting and scaling process that made the P-wave look smoother and allowed for easier identification of anomalies, such as faults, differing formations, and other unconformities. Then, the velocity of the P-wave was average causing a muting effect. This makes each time-depth interval averaged to create a clearer image for interpretation. Originally, each time-depth

interval is variable, and variability projects a fuzzy or chaotic image. After processing, the georectified data were entered into Kingdom Suite for interpretation.

Both the P-wave and SH-wave were processed with PC based software. Due to shallow distortions, Pugin (2005) applied his own routines for static correction analysis and modeling (operations 3, 4 and 8 in Table 4) (Pugin and Pullan, 2000). According to Pugin (2005) this near-surface correction process involves a very careful measurement of the initial arrival of the seismic signal (the first break) at each of the 24 channels recorded after each of the seismic record.

Table 3: P- and SH-wave acquisition parameters (Pugin, 2005)

	P-wave	SH-wave
Channels	24	12
Group interval	3 m	1.5 m
Geophone type	Vert. 40 Hz	Horiz. 14 Hz
Geophones/array		
Mounted on a sled	1	2
Shot interval	3 m	1.5 m
Source	15 kg	1 kg
(Sledge weight dropper,	hammer)	
Stack	1	3
Bin size	1.5 m	0.75 m
Max. fold	12	6
Recording system	Geode	Geode
Positioning system	Trimble DSM212H	Garmin 235
Sampling rate	0.125 ms	0.5 ms
Record length	0.3 s	1.024 s
DSP filters	LC: 35 Hz; HC: 1000 Hz	HC 250 Hz

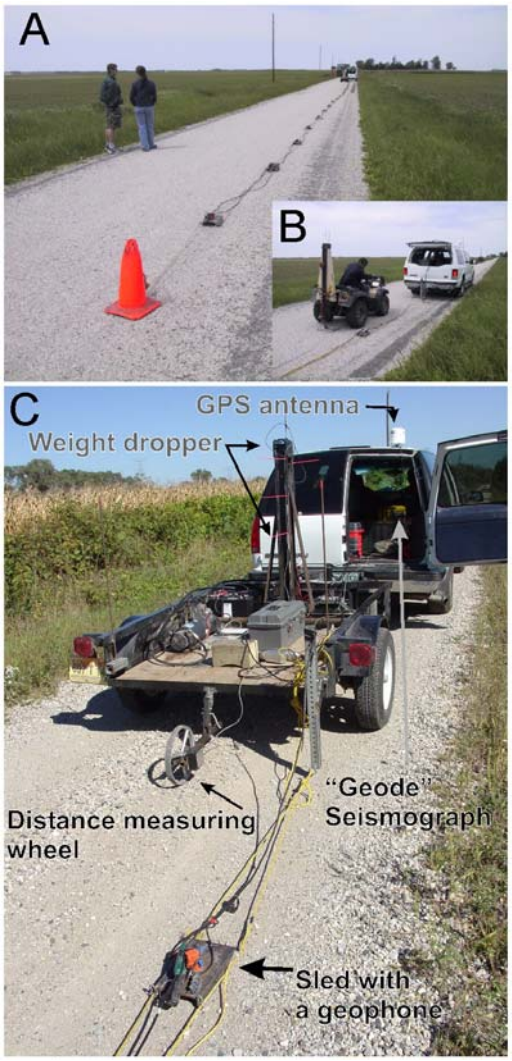

Figure 9: P-wave seismic reflection data acquisition using a landstreamer. A.The landstreamer on the road. B. ATV mounted weight-dropper. C. With the weight-dropper mounted on a trailer (Pugin, 2005).

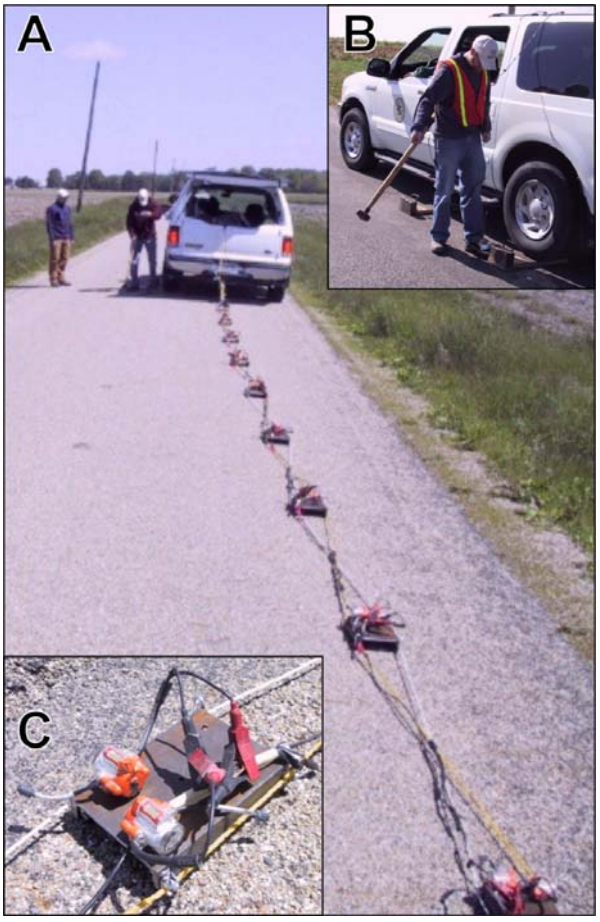

Figure 10: SH-wave seismic reflection data acquisition using a land streamer. A. The land streamer towed by the car. B. The horizontal impulsive hammer source. C. The sled with 2 opposing cross-connected geophones (Pugin, 2005).

Table 4. P-wave processing parameters

Data conversion SEG2 to SGY-KGS
Geometry edit
Trace edit
Refraction analysis and modeling for static correction calculation (*)
Band Pass filter 90-350 Hz
Mute remnant ground roll energy (bottom mute)
Time shift: static corrections application (*)
Velocity analysis
Normal Move Out correction
Stretch Mute (top mute)
AGC scaling 250 ms window
Residual static
Stack (divided by the square root of fold)
Spiking deconvolution 1% / 26 ms
Fold Balancing (**)
Phase shift migration using stack velocity analysis
Large Wavelength topographic static corrections on a datum (*)
Depth conversion using average velocities from borehole data
(*) see Pugin and Pullan (2000)
(**) see Pugin (2002)

Table 5. SH-wave processing parameters

Data conversion SEG2 to SGY-KGS
Geometry edit
AGC scaling: 50 ms window
Band Pass filter: 25-60 Hz
Mute remnant surface-wave energy (top mute)
Velocity analysis
Normal Move Out correction
Stretch Mute (top mute)
Stack
Fold Balancing (**)
Phase shift migration using stack velocity analysis
Large-wavelength topographic static corrections on a datum (*)
Depth conversion using average velocities from borehole data
(*) see Pugin and Pullan (2000)
(**)see Pugin (2002)

Results

The SH-wave seismic data was interpreted to determine lithological changes and structural discontinuities. Structural discontinuities refer to any structural anomaly interpreted within the SH-wave profiles, which includes man made and geologic.

Gamma ray – neutron well log data and borehole formation information were used to interpret the SH-wave profiles. There is a lack of core data to calibrate the well logs and there are no acoustic logs to calibrate the generated seismic profiles. However, time-depth intervals and seismic velocities were estimated for the purpose of interpretation for the different rock units. The same was done for the P-wave seismic data.

In Plate 1 the bedrock units captured in the SH-wave and P-wave seismic survey are shown in 2D and 3D maps. The Platteville Formation, the surficial bedrock unit in the northern portion of the field, is eroded away throughout most of the southern portion of the field excluding the southwest corner. The St. Peter Sandstone, stratigraphically below the Platteville Formation in the northern portion of the field, is the surficial bedrock unit in most of the south portion of the field. The St. Peter Sandstone is also eroded away, but just at the top of the dome in an elongated oval shape (Plate 1). The Shakopee Dolomite is present throughout the entire field just below the St. Peter Sandstone and is at the surface of the bedrock where the St. Peter Sandstone is eroded away. The New Richmond Sandstone underlies the Shakopee Dolomite throughout the entire field and is the last possible interpretable formation from the seismic survey.

The SH-wave profiles revealed a possible fault zone, many fracture zones, and confirmed the one major fault (Plate 1 and 2) that was already known to exist. In the southwestern corner of the seismic survey a fault zone was found revealing displacement

of up to 200 feet (Plate 1 and 2). Between the southernmost edge of the survey and the major fault, there exist several fractures or faults. North of the major fault, there are also many fractures. Even though fractures exist throughout, there are areas that are interpreted as fracture zones because of displacement through the zone. Otherwise, the faults and fractures are consistently present but not significant because of any other factors.

The P-wave profiles reveal a gas bubble that exists within more than one rock formation, as indicated by a bright area within the P-wave profile (Plate 2). The shape and size is suggestive of gas that is migrating upwards through the fractures and faults within the bedrock (Plate 2).

Also, north of the major fault, a gas bubble may exist, but the signal is not distinct enough to interpret. However, many fractures and fault zones exist within the northern portion of the seismic survey.

Discussion

The P-wave profiles have bright spots from the presence of gas within the shallow subsurface. The gas bubble is present most likely within the Shakopee Formation and the New Richmond Sandstone (Plates 1 and 2). The gas bubble pattern follows closely to the faults and fractures seen in Plate 2. The second P-wave and SH-wave profiles from the top exhibit these qualities excellently on the left hand side (south). These profiles were taken from the gathering system in the south to the gathering system in the north.

The SH-wave profiles were correlated with the corresponding P-wave profiles, where they were available. The result being that many of the faults and fractures in the

southern portion of the field directly correspond with the gas bubble suggesting that gas migration may be possible through the faults and fractures (Plate 2).

The SH-wave profile 1 from Plate 2 has a fracture zone that extends from 900 to 1600 meters (distance) with a vertical displacement of 200 feet. As for the rest of the structural discontinuities within SH-wave profile 1, they are most likely due to fracturing as a result of the structural deformation that has occurred in the area.

SH-wave profile 2 has structural discontinuities at 320 to 400 meters (distance) which are due to wells that were installed for injection and withdrawal. Also, a structural discontinuity by the P. Mathesius 5 and Wujek 1 are most likely associated with the wells. Otherwise, the other structural discontinuities are most likely associated with fractures.

SH-wave profile 3 exhibits a cluster of structural discontinuities between 2400 and 2800 meters (distance), which is probably a fracture zone. Also, there is a fault at 3000 meters (distance). Otherwise, the structural discontinuities are most likely fractures.

SH-wave profile 4, the only east-west profile on Plate 2, has a segment of data that is missing which caused the missing portion near the middle of the profile. As for the westerly portion of the profile, the Roulston 2 has been interpreted as a structural discontinuity, and a cluster of structural discontinuities have been interpreted between 550 and 750 meters (distance), which is a possible fracture zone with no apparent displacement. On the east side there is a fracture zone interpreted between 200 and 700 meters (distance). As for the rest, no other structural discontinuities are clear enough to be interpreted.

As for the P-wave profiles, all show the gas bubble clearly defined as the bright segments within each profile. On P-wave profile 1 the gas bubble is interpreted from around 700 meters on the first segment to the main fault all within the southern portion of the field. There are also possible faded and bright portions north of the fault. However, they are not clear enough for interpretation.

P-wave profile 2 has a bright segment caused by the gas throughout the entire portion of the profile south of the fault. As well, nothing is clear enough for interpretation north of the fault.

P-wave profile 3 shows evidence of the gas bubble by means of a bright spot on the profile throughout most of the profile south of the fault. Though there is an uninterpretable portion from 110 to 1300 meters (distance). In this case the north portion of the field was not surveyed, so whether gas exists near the surface in the northern portion of the field is not known.

P-wave profile 4 has a bright portion caused by the gas excluding 500 to 1100 meters in the second portion of the profile. The gas bubble to the east of this dead spot may not be gas from Nicor and could definitely be gas from biogenic processes beneath the surface. However, it has not been tested, and therefore, the gas's origin is not known.

CHAPTER V

SUMMARY, CONCLUSIONS, AND RECOMMENDATIONS

Summary of the Research Problem, Methods, and Findings

Due to reduced crop growth within a field near the southern portion of the gathering system within the underground gas storge field, and investigation of possible gas migration conduits was performed using well log analysis and a shallow high-resolution seismic survey. Well log analysis was used to determine whether structural deformation was existent within the reservoir. Also, porosities of every formation in and above the reservoir were calculated based on 3 newly drilled observation wells just outside the reservoir gas bubble to delineate whether structural deformation, causing a secondary porosity, may be playing a role in gas migration. A high-resolution seismic survey was also performed to delineate any shallow gas using P-wave seismic reflection and determines lithological features including faults, fractures, and rock formations using S-wave reflection data.

It was found that the reservoir itself has undergone a great deal of structural deformation. V_{sh} quantity surfaces exhibited that more data being available showed signs of greater heterogeneity. The data was krigged using Surfer, which caused a smoothing over effect where actual data was lacking. Data points that were the closest in proximity were the most different especially in the southern portion of the field.

The porosity data also yielded a possible conduit for gas migration. The Eau Claire Cap Rock (A Cap Rock), a siltstone, had porosities of up to 56% and had an average of 20 to 25% at all three boreholes.

The seismic survey pinpointed where the gas is being captured nears the surface (P-wave), but the gas bubble also showed signs of migration upwards. The S-wave reflection data delineated fractures, faults, and lithological changes within the bedrock. There was one major fault and many fault zones.

Conclusions and Implications

When all of the findings are combined, there is definitely a strong indication of fracturing and faulting throughout the field. However, the south of the major fault gas has been found at the surface and in the near surface bedrock. The V_{sh} exhibits structural deformation, which cannot be ruled out as a potential conduit for gas migration. Additionally, the porosity of the Eau Claire Cap Rock (A Cap Rock) is too high to disregard as a possible migration pathway out of the reservoir. The high-resolution seismic reflection data revealed a gas bubble of unknown concentration near the surface. Also faults and fractures seemed to be associated with a great portion of the gas bubble. The possible migration pathways have been found. North of the fault, gas was not found near the surface in the seismic profiles. Yet, possible migration pathways were found and units and formations with large storage capacities were established. The units and formations with large storage capacities were not delineated by the seismic survey because of their depth. The seismic equipment used for the seismic survey were did not have the capacity to capture depth of 700 to 100 feet. Therefore, more data is needed.

The gas storage field may have gas migration from the reservoir to the surface. Yet, it should be noted that mechanical problems within the wells may be supplying the gas bubble in the south portion of the field. The south portion of the gathering system is the oldest. It was developed at the same time as the reservoir was being developed. However, the north portion of the gathering system is not much younger.

Concerning the seismic reflection data, the actual location, time-depth interval, to define the seismic velocities and delineate the actual depth of the gas bubble and rock formations has not been completed. Once the seismic velocities are established, a picture of the gathering system overlain on the P-wave seismic profiles may help determine if and how much the gathering system is contributing to the gas bubble and gas migration.

Recommendations for Future Research

Further investigation of the glacial till, ground truthing of the seismic survey, and coring of the bedrock with core analysis are just a few of the avenues of research that could be pursued in the future. Also, a more complete seismic survey, a follow up on the P-wave to complete a time lapse seismic survey, a three dimensional survey, or a seismic survey that is capable of capturing deeper elements of the bedrock are all possible opportunities for research.

A thorough investigation of the effects of the reservoir on its overlying bedrock is also a definite avenue of research. If the reservoir pressure is exceeding the equilibrium pressure of the aquifer every year, is this causing too much stress and strain on the overlying bedrock. Pressure transducers could be used to gauge the amount of stress and

strain that is exerted on the overlying bedrock every year during the time that peak capacity is completed.

REFERENCES

Batzle, M. and Wang, Z., Seismic Properties of Pore Fluids, Geophysics, v. 57, no. 11, November 1992, 1396-1408.

Blondin, E. and Mari, J.L., Detection of Gas Bubble Boundary Movement, Geophysical Prospecting, vol. 34, (1986), p. 73-93.

Bond, D.C., Hydrodynamics in Deep Aquifers of the Illinois Basin, Illinois State Geological Survey, Circular 470, 1972.

Buschbach, T.C. and Bond, D.C., Underground Storage of Natural Gas in Illinois, Illinois State Geological Survey, Illinois Petroleum 101, 1973.

Dake, L.P., 1978, Fundamentals of reservoir Engineering, Elsevier Scientific Publishing Company, New York, 156-189.

Deters, J., Fugate, M., Schofield, K., Hammerschmidt, A., and Sanders, A., September – December 2003, Personal Communication, Nicor, Inc., 1844 Ferry Road Naperville, Illinois 60563**.**

Doveton, J.H., Borehole Petrophysical Chemostratigraphy of Pennsylvannian Black Shales in the Kansas Subsurface, Chemical Geology, 206 (2004), p. 249-258.

Doveton, J.H., 1994, Geologic Log Analysis Using Computer Methods, American Association of Petroleum Geologists Computer Applications in Geology, No.2.

Dresser Atlas, Well Logging and Interpretation Techniques, Dresser Industries, Inc., 1982, p. 79-83.

Energy Information Administration (EIA), Department of Energy, 2004, http://www.eia.doe.gov/pub/oil_gas/natural_gas/analysis_publications/storagebasics/storagebasics.html

Energy Information Administration (EIA), Department of Energy, 2005, http://tonto.eia.doe.gov/dnav/ng/ng_sum_lsum_dcu_nus_m.htm

Enquist, B.E., Troy Grove Storage Reservoirs: A geologic evaluation of the complex faulted inter-relationship of the storage zones, Report for Northern Illinois Gas Company, April 1968, 1-20.

Fertl, W.H., and Chilingarian, G.V., Type and Distribution Modes of Clay Minerals from Well Logging Data, Journal of Petroleum Science and Engineering, 3 (1990), p. 321-332.

Harrigan, S.J., and Lackie, J., 2003, Mud Logs of HCCC 1, Krenz 2 and Hochstatter 2.

Hester, T.C., Prediction of Gas Production Using Well Logs, Cretaceous of North-Central Montana, The Rocky Mountain Association of Geologists, The Mountain Geologist, v. 36, no. 2 (April 1999), p.85-98.

Jorgenson, D., 1989, Using geophysical logs to estimate porosity, water resistivity, and intrinsic permeability, United States Geological Survey Water-Supply Paper, 2321.

Katz, D. and Coats, K., 1968, The Underground Storage of Fluids, Malloy Lithographing, Inc. 1-200.

Keen, G., The Underground Storage of Natural Gas, Thirty-fourth Annual Tri-State Field Conference, October 2-4, 1970, Sponsored by the Department of Geology Northern Illinois University, Dekalb, Illinois, 32-33.

Kerr, S.A., Grau, J.A., and Schweitzer, J.S., A comparison between elemental logs and core data, *Nuclear Geophysics*, v. 6, no. 3 (1992), p. 303-323.

McGinnis, L., Heigold, P., Ervin, C., and Heidari, M. The Gravity Field and Tectonics of Illinois, Illinois State Geological Survey, Circular 494, 1976, 1-28.

Mills, W.R., Stromswold, D.C., and Allen, L.S., Advances in Nuclear Oil Well Logging, Nuclear Geophysics, v. 5, no. 3 (1991), p. 209-227.

Minette, D., Utilizing MWD Geometry and Innovative Neutron Detection Techniques to Minimize the Effects of Thermal Neutron Absorbers on Log Response, SPWLA 39th Annual Logging Symposium, May 26-29, 1998.

Nelson, W.J., 1995, Structural Features In Illinois, Department of Natural Resources, Illinois State Geological Society, Bulletin 100, p. 72-120.

Nissen, S.E., Watney, W.L., and Xia, J., High-Resolution Seismic Detection of Shallow Natural Gas Beneath Hutchinson, Kansas, Environmental Geosciences, vol. 11, no. 3 (September 2004), p. 129-142.

Pugin, A, 2005, Personal Communication, Illinois State Geological Survey, 612 Peabody Drive, Champaign, Illinois 61820

Pugin, A. and Pullan, S.E., First-Arrival alignment static corrections applied to shallow seismic reflection data. Journal of Environmental & Engineering Geophysics, vol. 5, no. 1, 2000, p. 7-15

Vidal, S., Longuemare, P., Huguet, F., and Mechler, P., Reservoir Parameters Quantification from Seismic Monitoring Integrating Geomechanics, Oil and Gas Science and Technology, Rev. IFP, vol. 57, no. 5 (2002), p. 555-568.

Vidal, S., Longuemare, P., and Huguet, F. Integrating Geomechanics and Geophysics for Reservoir Seismic Monitoring Feasibility Studies, paper presented at the 2000

Society of Petroleum Engineers European Petroleum Conference, Paris, France, October 24-25, 2000.

Willman, H., Atherton, E., Buschbach, T., Collinson, C., Frye, J., Hopkins, M., Lineback, J., and Simon, J. Handbook of Illinois Stratigraphy, Illinois State Geological Survey, Bulletin 95, 1975, 34-46.

APPENDIX A

WELL LOG AND SEISMIC SURVEY TERMS

Well Log Terms

Abbreviation	*Definition*
Vsh	Volume of Shale
PHIE	Effective Porosity
PHIA	Average Porosity
PHID	Density Porosity
RHOB	Bulk Density
NU91	Neutron counts in API Units in 1991 (year example)
GR	Gamma Ray
SP	Spontaneous Potential

Seismic Survey Terms

Abbreviation	*Definition*
P-Wave	Primary wave
SH-Wave	Shear Horizontal Wave

APPENDIX B

TABLE OF VOLUME OF SHALE CALCULATIONS

Table 1: Volume of Shale Calculations

Well Name	A Cap	A Sand	B Cap	B Sand	C Cap	C Sand	Mt. S Cap	Mt. Simon
Amfahr 5 (N)	0.669	0.264	0.689	0.221	0.654	0.38	0.673	0.235
Amfahr 11 (N)	0.578	0.238	0.697	0.118	0.664	0.325	0.818	0.153
Amfahr 13 (N)	0.417	0.125	0.552	0.092	0.475	0.313	0.596	0.17
Amfahr 15 (N)	0.575	0.191	0.733	0.141	0.628	0.32	0.814	0.2
Amfahr 27 (N)	0.642	0.217	0.768	0.212	0.576	0.395	0.734	0.345
Amfahr 29 (N)	0.565	0.165	0.706	0.126	0.58	0.244	0.694	0.19
Becker 1 (N)	0.593	0.193	0.726	0.155	0.604	0.307	0.697	0.233
Schmidt 1 (N)	0.707	0.238	0.723	0.221	0.703	0.345	0.691	0.24
Whitlock 1 (N)	0.663	0.141	0.691	0.16	0.495	0.262	0.734	0.214
Whitmore 1 (N)	0.651	0.136	0.697	0.175	0.687	0.164	0.692	0.29
Hamer 3 (S)	0.571	0.194	0.705	0.343	0.67	0.36	0.781	0.152
Hoffman 3 (S)	0.677	0.2	0.708	0.385	0.642	0.319	0.801	0.235
Hoffman 6 (S)	0.695	0.145	0.744	0.084	0.668	0.283	0.772	0.194
Hoffman 11 (S)	0.607	0.281	0.727	0.201	0.719	0.411	0.812	0.268
Klinefelter 1 (S)	0.713	0.109	0.697	0.255	0.527	0.247	0.622	0.168
L Mathesius 1 (S)	0.666	0.148	0.705	0.164	0.699	0.326	0.763	0.269
L. Mathesius 3 (S)	0.59	0.146	0.716	0.133	0.672	0.24	0.818	0.169
LSNB 1 (S)	0.665	0.131	0.662	0.264	0.658	0.307		
Murphy 1 (S)	0.653	0.225	0.716	0.111	0.653	0.353	0.754	0.243
P. Mathesius 2 (S)	0.644	0.208	0.703	0.164	0.652	0.251	0.645	0.112
P. Mathesius 9 (S)	0.601	0.14	0.712	0.109	0.635	0.28	0.735	0.199
P. Mathesius 13 (S)	0.644	0.203	0.776	0.151	0.656	0.288	0.762	0.216
P. Mathesius 14 (S)	0.547	0.184	0.696	0.2	0.658	0.372	0.778	0.328
P. Mathesius 17 (S)	0.58	0.151	0.744	0.148	0.523	0.246	0.63	0.131
Roulston 2 (S)	0.638	0.198	0.656	0.085	0.636	0.346	0.804	0.164
Roulston 4 (S)	0.532	0.163	0.561	0.083	0.654	0.259	0.653	0.245
Weldon 3 (S)	0.569	0.215	0.558	0.13	0.603	0.329	0.763	0.275
Weldon 16 (S)	0.624	0.312	0.737	0.261	0.664	0.314	0.738	0.269
Weldon 18 (S)	0.402	0.176	0.647	0.211	0.614	0.325	0.708	0.353
Total Averages	0.610	0.187	0.695	0.176	0.630	0.307	0.732	0.224
Standard Deviation	0.073617	0.049006	0.055596	0.074442	0.061057	0.05453	0.064448	0.062043